

Colloid Population Heterogeneity Drives Hyperexponential Deviation from Classic Filtration Theory

MEIPING TONG AND
WILLIAM P. JOHNSON*

Department of Geology and Geophysics, The University of Utah, Salt Lake City, Utah 84112

The deposition behaviors of carboxylate-modified polystyrene latex microspheres (six sizes ranging from 0.1 to 2.0 μm) in packed porous media (soda-lime glass beads) were examined under a variety of environmentally relevant pore fluid velocities (4–8 $\text{m}\cdot\text{day}^{-1}$) in the presence of an energy barrier to deposition. Hyperexponential profiles of retained colloids were observed for all microsphere sizes (0.1–2.0 μm) at two fluid velocities (4 and 8 $\text{m}\cdot\text{day}^{-1}$). Experiments with columns in series demonstrated for three distinct sizes of microspheres that colloid population heterogeneity drove hyperexponential deviation from filtration theory. A significant portion of retained colloids was released upon introduction of low ionic strength solution, indicating that the majority of colloids were retained via secondary energy minima. However, there was no preferential re-entrainment of secondary minimum-associated colloids near the column inlet, indicating that the hyperexponential deviation from classic filtration theory was not due to deposition in the secondary energy minimum.

Introduction

Colloid transport in porous media is commonly described by classic clean bed filtration theory (1–3), in which a spatially constant first-order deposition rate coefficient is estimated based on the physical attributes of the system. For a system absent an energy barrier (opposite-charged colloids and grain collector), the colloid deposition rate coefficients are invariant with transport distance, and one observes log linear decreases in mobile and retained colloid concentrations (C) with increasing distance (x) from source (log-linear retained profiles) (1, 4, 5), as shown in the following mathematical relationship which can be derived from the advection-dispersion-deposition equation, under the assumption that dispersion is negligible

$$\ln \frac{C}{C_0} = -\frac{k_f}{v}x \quad (1)$$

where C is the colloid concentration at some distance (x), C_0 is the colloid concentration at the source, k_f is the colloid deposition rate coefficient, and v is the fluid velocity.

In the presence of an energy barrier to deposition (like-charged colloids and collectors), colloid deposition rate coefficients are commonly reported to decrease with increasing transport distance, that is, the concentrations of

retained colloids decrease with distance from source faster than the log-linear rate expected from a spatially invariant deposition rate coefficient. In some systems, the observation of these hyperexponential decreases of retained and mobile colloid concentrations with distance has been linked to changes in collector properties along the flow path (6–8). However, in most cases, the hyperexponential profiles are observed in repacked porous media, where properties are evenly distributed along the flow path. Hence, the observed hyperexponential retained profiles have been largely attributed to distributions in surface properties among the colloid population (9–13), since relatively “sticky” colloids (colloids with relatively fast deposition rate coefficients) would be retained up-gradient of less-sticky colloids, producing a decrease in average deposition rate coefficient with increasing transport distance.

Other possible mechanisms of producing the observed hyperexponential deviation from filtration theory have recently been proposed. For example, Bradford et al. (14–17) hypothesized that physical straining was an important contributor to the observed hyperexponential deviations from classic filtration theory, since entrapment of colloids in “dead-end” pores can be reasonably expected to occur during movement of the colloid suspension from the surface (where fluid flow is evenly distributed across the pore domain) to the interior (where fluid flow is constrained to continuous pores). However, for most investigations, the colloid:collector diameter ratio was well below traditionally suggested ratios that would lead to straining, e.g., 0.05 (18, 19), and was also well below the recently suggested threshold ratio of 0.005 by Bradford et al. (15), suggesting that straining is not the major mechanism driving the hyperexponential retained profiles.

Tufenkji and Elimelech (20) recently attributed hyperexponential deviation from classic filtration theory to heterogeneity in surface characteristics either among the colloid population or on the porous media grains, prompting Johnson and Li (21) to comment that collector heterogeneity in a repacked bed cannot by itself generate the observed deviation but can possibly amplify the distribution induced by heterogeneity among the colloid population. Furthermore, Tufenkji and Elimelech (20) suggested that the fraction of the colloid population with fast deposition rate coefficients was deposited in the secondary energy minimum.

Assuming that the observed hyperexponential deviation is derived from a distribution of interaction energies among the colloid population, then the colloids exiting the packed porous media column should show less favorable interaction potentials (less sticky) relative to those entering the column. If transport experiments were conducted within porous media columns in series, then the retained colloid profile in the down-gradient column should yield lesser deposition rate coefficients and lesser deviation from filtration theory relative to the up-gradient column. Furthermore, since the magnitude of the log-linear retained colloid profile decreases with decreasing C_0 , a parallel porous media column having C_0 similar to the down-gradient column should show much greater hyperexponential deviation from filtration theory relative to the down-gradient column. Finally, elution of reversibly deposited microspheres with low ionic strength solution to re-entrain secondary minimum-associated colloids should indicate whether secondary minimum-associated colloids are retained preferentially in the up-gradient portion of the column, where colloids with fast deposition rate coefficients should be deposited.

The objective of this paper is to present colloid transport experiments with columns in series in order to demonstrate

* Corresponding author phone: (801) 581-5033; fax: (801) 581-7065; e-mail: wjohnson@mines.utah.edu.

that heterogeneity among the colloid population drives hyperexponential deviation from filtration theory. This result is shown for three distinct sizes of microspheres. Furthermore, we demonstrate that although the majority of colloids were associated with grain surfaces via the secondary energy minimum, there was no preferential re-entrainment of secondary minimum-associated colloids near the column inlet, indicating that the hyperexponential deviation from classic filtration theory was not due to deposition in the secondary energy minimum.

Method

Microspheres. Spherical fluorescent carboxylate-modified polystyrene latex microspheres (Molecular Probes, Inc., Eugene, OR) of six sizes (diameters of 0.1, 0.2, 0.5, 1.0, 1.1, and 2.0 μm , with negative surface charge densities of 0.3207, 0.282, 0.1419, 0.0175, 0.18, and 0.1076 mequiv g^{-1} , respectively) were used in all experiments. The 0.1, 0.2, 0.5, 1.0, 1.1, and 2.0 μm microsphere stock suspensions had particle concentrations of 3.6×10^{13} , 4.5×10^{12} , 2.9×10^{11} , 2.7×10^{10} , 2.7×10^{10} , and 4.5×10^9 microspheres mL^{-1} , respectively. The stock solutions contained NaN_3 (2 mM), whereas the 2.0 μm microsphere stock suspension also included 0.01% Tween-20.

Prior to injection, stock solutions for the 0.1, 0.2, 0.5, 1.0, and 1.1 μm microspheres were diluted in NaCl solution to achieve a nominal influent concentration (C_0) of $1.0 \times 10^7 \pm 30\%$ particles mL^{-1} at the desired ionic strength (NaCl), plus MOPS buffer (2.2 mM), yielding a solution pH of 6.72. The stock solution for the 2.0 μm microspheres was first diluted 10 times in pure (Milli-Q) water (Millipore Corp. Bedford, MA) and was washed three times to remove Tween-20. Washing involved centrifugation (10 000g for 10 min at 4 °C), followed by decanting and addition of pure water. Following washing, the 2.0 μm microsphere solution was diluted in NaCl solution to achieve a nominal influent concentration (C_0) of $1.0 \times 10^6 \pm 30\%$ at the desired ionic strength (NaCl) plus MOPS buffer (2.2 mM), yielding a solution pH of 6.72. Experiments were conducted at an ionic strength of 0.02 M for 0.1, 0.2, 0.5, and 1.0 μm microsphere sizes and at an ionic strength of 0.05 M for 2.0 μm microspheres except as noted.

Porous Media. Spherical soda lime glass beads (Cataphote Inc. Jackson, MS) with sizes ranging from 417 to 600 μm were used for microsphere deposition experiments in porous media. The procedure used for cleaning the glass beads is provided in previous publications (22).

Experimental Conditions. Cylindrical Plexiglass columns (20 cm long, 3.81 cm inner diameter) were dry-packed with glass beads, flushed with CO_2 , and equilibrated with microsphere-free solution. The procedure of packing and pre-equilibration is described in previous publications (22).

After pre-equilibration, a solution with microspheres was injected (3 pore volumes). This was followed by elution with microsphere-free solution (7 pore volumes). Selected experiments were eluted by low ionic strength solution (0.0002 M) (without microspheres) (7 pore volumes). The low ionic strength solution was introduced to eliminate the secondary energy minimum.

During injection, the microsphere suspension reservoirs were sonicated for 1 min per hour to minimize aggregation, as verified by flow cytometric analyses. The flow rate was varied between experiments to produce pore water velocities at 4 and 8 $\text{m}\cdot\text{day}^{-1}$. The suspensions and solutions were injected in up-flow mode using a syringe pump (Harvard Apparatus, Inc. Holliston, MA).

Sample Collection and Analysis. Column effluent samples were collected in 5 mL polystyrene tubes using a fraction collector (CF-1, Spectrum Chromatography, Houston, TX). Following the experiment, the sediment was dissected into

ten 2 cm-long segments, as the sediment was released from the column under gravity. Retained colloids were recovered by placing sediment segments (2 cm) into specified volumes of Milli-Q water and sonicating for 1 min, followed by manual vigorous shaking for half min. Aqueous effluent samples, and supernatant samples from recovery of retained microspheres, were analyzed using flow cytometry (BD FACScan, Becton Dickinson & Co., FranklinLakes, NJ) at a flow rate of $12 \mu\text{L}\cdot\text{min}^{-1}$ at an excitation wavelength of 488 nm and were counted for 1 min. Conversion of counts on the flow cytometer to microsphere concentrations was made using a calibration curve based on serial dilutions of microsphere suspensions of known concentration. The R^2 of the log-log calibration curves were consistently greater than 0.990. The area under the breakthrough-elution curve was integrated to yield the percentage of microspheres that exited the column. The percent of injected microspheres recovered from the sediment was determined by summing the number of microspheres recovered from all segments of the sediment and dividing by the total number injected. The overall recovery (mass balance) of microspheres was determined by summing the percentages of microspheres that exited and that were retained in the column. Mass recoveries (total from effluent and sediment) were all between 81% and 108%, with the majority between 88% and 105% recovery (Table 1). The excellent mass balance shows that the microspheres were detached by dilution into pure water, indicating that their mechanism of attachment was eliminated either by disassembling the pore structure or by increasing the magnitude of colloid-collector electrostatic repulsion.

Particle Tracking Model. The transport and retention of microspheres was modeled using an advection-dispersion equation that includes removal from, and re-entrainment to, the aqueous phase

$$\frac{\partial C}{\partial t} = -v\frac{\partial C}{\partial x} + D\frac{\partial^2 C}{\partial x^2} - k_f C + \frac{\rho_b}{\theta} k_r S_r \quad (2)$$

where C is the concentration of microspheres in the aqueous phase (microspheres per unit volume of fluid), t is the travel time, x is the travel distance, v is the flow velocity, D is the dispersion coefficient of the colloid particles, θ is the porosity, ρ_b is the bulk density of sediment, and k_f and k_r are rate coefficients for microsphere deposition to and re-entrainment from the solid phase, respectively. S_r is the reversibly retained microsphere concentration on the solid phase (microspheres per unit mass of sediment) and can be further expressed as

$$S_r = f_r S \quad (3)$$

where S is the total deposited microsphere concentration, and f_r is the fraction of reversibly retained microspheres.

A one-dimensional discrete random-walk particle-tracking model was used to solve eq 2 under the conditions of the column experiments, and details of implementation of the governing equation are given in other publications (22–24). It is important to note that the probabilistic approach used in the particle tracking model decouples the parameters k_f and f_r , whereas this decoupling is not apparent in the equations as written in continuum form (eqs 2 and 3).

A distribution of deposition rate coefficients among the population of colloids was simulated according to strategy employed by Li et al. (22). The log-normal distribution was represented by a mean $\ln k_f$ and standard deviation ($\sigma \ln k_f$), where the standard deviation represents the degree of deviation from classic filtration theory (log-linearity). Parameter values from the particle tracking simulations were obtained by best fits to both the colloid breakthrough-elution curves and the profiles of retained colloids. The mass balance

TABLE 1. Porous Media Experimental Conditions, Mass Balances, and Model Parameters for Simulations Using the Particle-Tracking Model^a

size (μm)	IS (M)	vel (m-day^{-1})	% rec	% sed	single deposition rate coefficient			distributed deposition rate coefficient			
					k_f (h^{-1})	k_r (h^{-1})	f_r	mean $\ln k_f$ (h^{-1})	k_f (h^{-1})	$\sigma \ln k_f$	f_r
0.1	0.02	4	86.0	35.2	0.72	0.10	0.07	26.5	0.10	4.20	0.30
		8	101.1	2.2	0.06	0.45	0.40	0.42	0.45	4.53	0.60
0.2	0.02	4	93.1	22.2	0.26	0.15	0.30	8.33	0.05	4.81	0.97
		8 ^{up}	105.2	14.6	0.25	0.50	0.03	3.41	0.65	4.96	0.11
		8 ^{down}	89.0	12.0	0.19	0.33	0.12	0.36	0.33	2.01	0.15
		8 ^{parallel}	105.5	11.8	0.25	0.65	0.04	3.97	0.65	5.92	0.15
0.5	0.02	4	99.9	3.6	0.063	0.20	0.40	0.49	0.20	3.83	0.60
		8	100.0	2.2	0.06	0.48	0.38	0.37	0.48	4.34	0.52
1.0	0.02	4	87.7	17.0	0.25	0.30	0.42	3.42	0.30	4.28	0.68
1.1	0.01	8	100.1	7.9	0.17	0.50	0.21	1.59	0.50	4.31	0.40
		4 ^{up}	101.2	21.7	0.25	0.35	0.14	4.28	0.35	3.96	0.38
2.0	0.05	4 ^{down}	91.5	2.4	0.03	0.20	0.35	0.097	0.20	3.03	0.55
		4 ^{parallel}	99.1	8.4	0.12	0.25	0.30	2.97	0.25	5.96	0.30
		8 ^{up}	104.1	51.3	1.20	0.70	0.03	5.50	0.70	2.00	0.05
		8 ^{down}	91.6	25.5	0.58	0.80	0.13	1.01	0.82	1.51	0.15
		8 ^{parallel}	98.2	46.6	1.20	0.70	0.07	5.61	0.70	2.09	0.13
		4	93.3	59.2	0.92	0.10	0.02	7.01	0.10	1.99	0.05
2.0	0.05	8 ^{up}	92.7	26.3	0.56	0.11	0.10	1.01	0.11	1.51	0.10
		8 ^{down}	81.1	11.7	0.26	0.11	0.10	0.26	0.11	0	0.10
		8 ^{parallel}	88.9	16.4	0.53	0.11	0.10	1.01	0.11	1.51	0.10

^a "Size" refers to colloid diameter, "IS" indicates ionic strength (M), "vel" indicates pore water velocity (m-day^{-1}), "% rec" refers to average percent recovery of injected microspheres via effluent plus via desorption following dissection, and "% sed" refers to percent recovery of injected microspheres via desorption following dissection. The parameter k_f is the deposition rate coefficient, and the parameters k_r and f_r are the re-entrainment rate coefficient and the fraction of reversible deposition, respectively. The parameters "mean $\ln k_f$ " and " $\sigma \ln k_f$ " are the mean and standard deviation of the log-normal distribution of deposition rate coefficients, respectively. The terms "up", "down", and "parallel" designate up-gradient, down-gradient, and parallel columns, respectively.

was honored by forcing the simulations to match the distribution of colloids among the aqueous and sediment phases, as determined from the experiments. The relatively small mass that was unaccounted (or overaccounted) for in the mass balance was arbitrarily reappportioned (or removed equally) (as percent) to (or from) the effluent and sediment by multiplying the number of colloids in those phases by an equivalent factor in order to close the mass balance.

Results

The retained microsphere concentrations decreased faster than exponential as a function of transport distance (Figure 1A,B), indicating that the deposition rate coefficients decreased with increasing transport distance. As described above, a spatially constant deposition rate coefficient would yield a log-linear retained colloid profile. That the profiles shown in Figure 1 are hyperexponential is demonstrated by comparison to log-linear profiles developed using a single deposition rate coefficient that honored the mass balances, as shown in the Supporting Information.

These hyperexponential profiles of retained colloids were observed for all microsphere sizes (0.1–2.0 μm) at the two fluid velocities examined (4 and 8 m-day^{-1}) (Figure 1A,B), consistent with many previous observations for both biological and nonbiological colloids both in the field and in the laboratory. No blocking or ripening occurred during the experiments, as indicated by the constant steady-state breakthrough plateaus for all microsphere sizes at both 4 and 8 m-day^{-1} (Figure 2).

To examine the possibility that the observed hyperexponential profiles were driven by a distribution of interaction energies among the colloid population, experiments with columns in series were performed for three microsphere sizes (0.2, 1.1, and 2.0 μm). As well, parallel columns with C_0 equal to 1/3 of the up-gradient columns were also examined for each microsphere size. The up-gradient and down-gradient columns were connected using Teflon tubing and a 3-way

valve, which allowed sampling of small fraction of the effluent (~3% of flow) from the up-gradient column, which also served to quantify the influent concentration entering the down-gradient column.

The retained profiles from serial injection and parallel experiments for three microsphere sizes (0.2, 1.1, and 2.0 μm) and an ionic strength of 0.02 M and fluid velocity of 8 m-day^{-1} are shown in Figure 3 (A–C). The retained profiles from the parallel (reduced C_0) columns were lower in magnitude by a factor of 3 relative to those of the up-gradient columns (Figure 3), indicating that the deposition rate coefficient was independent of the influent concentration under the range examined. The retained colloid profiles from the up-gradient and parallel columns showed very similar shapes (Figure 3), demonstrating that the difference in the influent concentration did not affect the shapes of the retained colloid profiles. In contrast, the shapes of the retained colloid profiles were affected by transport, as shown by the relatively flat profiles from the down-gradient columns (Figure 3). This observation held true for all three microsphere sizes examined. The result was also repeated for the 1.1 μm microspheres at a factor of 2 lower fluid velocity (4 m-day^{-1}) (Figure 4).

Close inspection of the retained profile from the down-gradient column (2.0 μm microspheres) indicated that segments near the column outlet displayed increased retained colloid concentrations relative to preceding segments, possibly due to colloid redeposition. This increase of colloid concentration near column outlet has also been observed in experiments where deposited colloids were remobilized via both ionic strength and pH perturbations (unpublished data).

Discussion

In the presence of an energy barrier to deposition, colloid deposition efficiencies as a function of colloid size cannot be expected to follow the trend predicted by filtration theory, as demonstrated in Tong and Johnson (25). The lack of

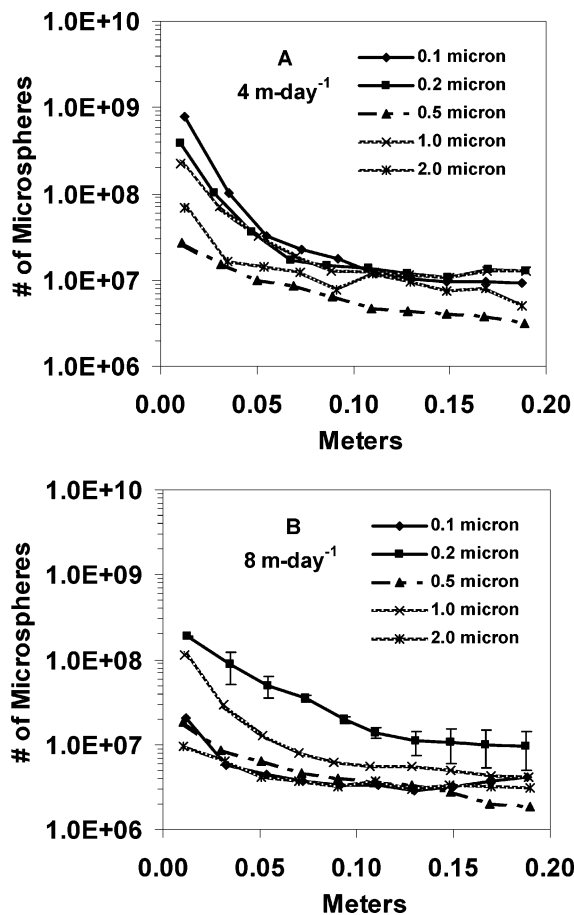


FIGURE 1. Retained profiles for different microsphere sizes (0.1–2.0 μm) at fluid velocity of 4 $\text{m}\cdot\text{day}^{-1}$ (A) and 8 $\text{m}\cdot\text{day}^{-1}$ (B) at an ionic strength = 0.02 M and pH = 6.72 (ionic strength = 0.05 M for the 2.0 μm microspheres).

correspondence to filtration theory in the presence of an energy barrier to deposition may result from differences in surface characteristics among the colloid population. Therefore, our goal in examining retained colloid profiles for a range of colloid sizes was not to demonstrate trends as a function of colloid size but rather to demonstrate that deviation from classic filtration theory was consistently observed across a range of colloid sizes and to demonstrate that the effect of transport on the corresponding retained colloid profiles was consistent across the range of colloid sizes.

Observed deviation from classic filtration theory (deviation from log-linear retained colloid profiles) nominally appears to be less for experiments performed at higher fluid velocity relative to those performed at lower fluid velocity, as indicated by the increasing log-linearity of the retained profiles with increasing fluid velocity (Figure 1A,B). However, this apparent influence of fluid velocity is an artifact that results from decreases in the deposition rate coefficients and concomitant decreases in the slope of the retained colloid profile, with increasing fluid velocity, as demonstrated in previous publications (5, 26–28). The deviation from classic filtration theory is more objectively quantified by determining the standard deviation of the deposition rate coefficient ($\sigma \ln k_f$) determined from the particle simulations. As shown in Table 1, the value of $\sigma \ln k_f$ was similar for the two fluid velocities for all colloid sizes examined except for the 1.1 μm microspheres where the fluid velocity change was accompanied by an ionic strength change.

The independence of deposition rate coefficients and influent concentrations under the range examined is shown

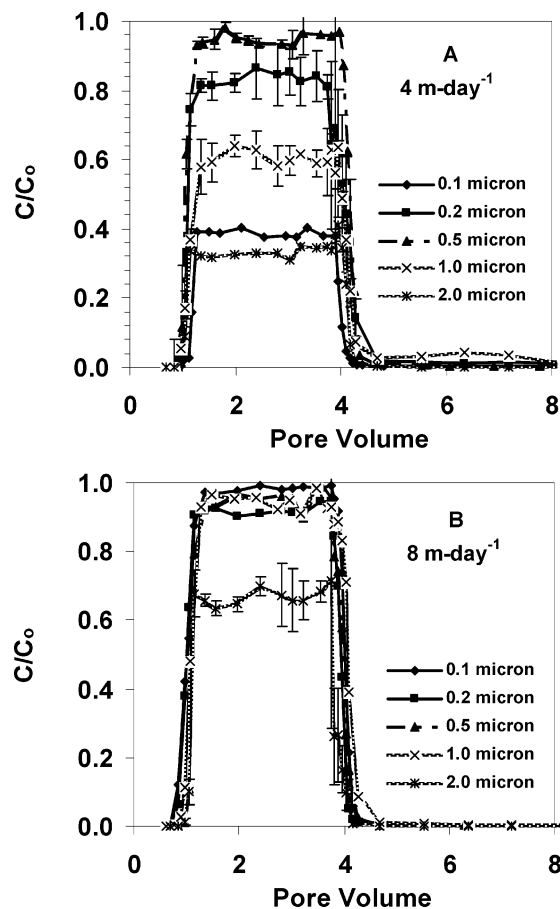


FIGURE 2. Breakthrough curves for different microsphere sizes (0.1–2.0 μm) at fluid velocity of 4 $\text{m}\cdot\text{day}^{-1}$ (A) and 8 $\text{m}\cdot\text{day}^{-1}$ (B) at an ionic strength = 0.02 M and pH = 6.72 (ionic strength = 0.05 M for the 2.0 μm microspheres).

by the similar values of mean $\ln k_f$ among the up-gradient and parallel columns (Table 1). The similar shapes of the up-gradient and parallel retained profiles are quantified by the very similar values of $\sigma \ln k_f$ among the up-gradient and parallel columns (Table 1). The kinetic simulations demonstrate that the retained colloid profiles from the up-gradient and parallel columns were characterized by similar mean and distributions in deposition rate coefficients. In contrast, the down-gradient columns showed reduced values of mean $\ln k_f$ and reduced values of $\sigma \ln k_f$ (Table 1) relative to the up-gradient and parallel columns, indicating that the distribution of deposition rate coefficients characterizing the down-gradient columns had a reduced mean and narrower distribution relative to the up-gradient and parallel columns. These observations strongly indicate that stickier individuals in the population were removed in the up-gradient column and that the population became less sticky with increasing transport distance. Representative simulations using both single and distributed deposition rate coefficients are provided in the Supporting Information.

Our conclusion is consistent with previous bacterial transport experiments involving two columns in series (11) where no deposition was observed in the down-gradient columns, and it was concluded that the colloid population became less sticky with increasing transport distance. Although many authors have previously attributed hyper-exponential deviation to heterogeneity among the colloid population, some authors have indicated that such heterogeneity is insufficient to produce the wide distributions in interaction energies necessary to generate the observed deviations (e.g., ref 20). Multiple potential sources of colloid

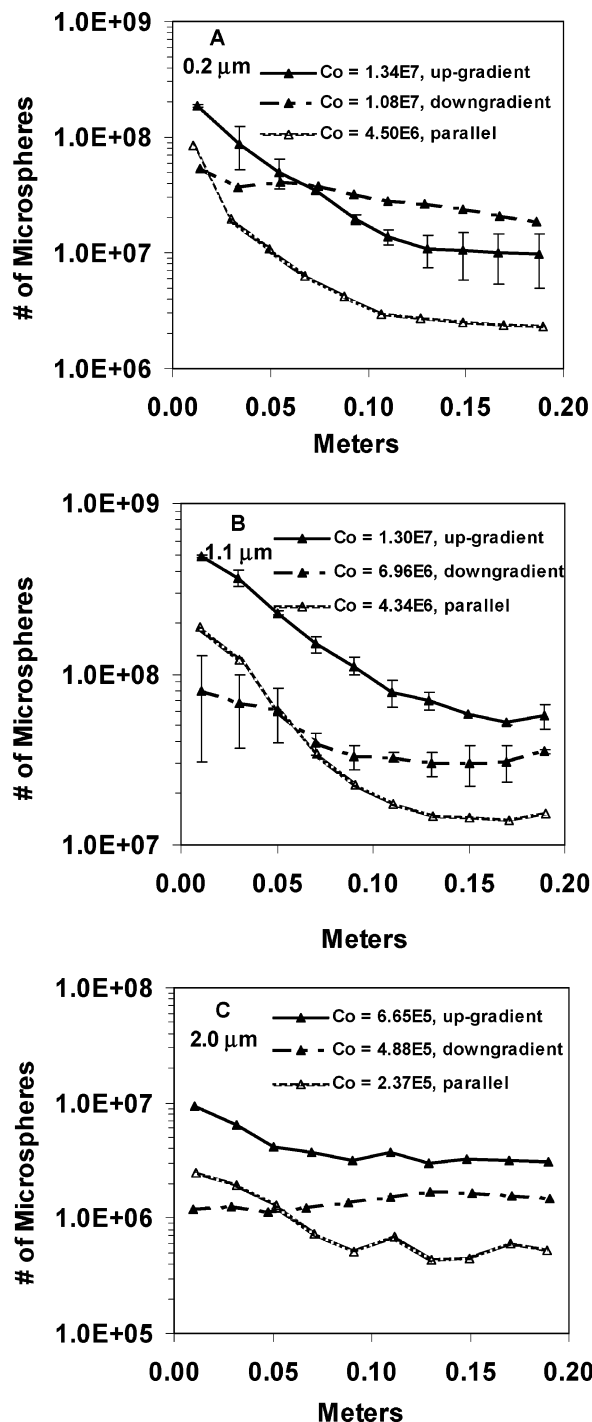


FIGURE 3. Retained profiles for the 0.2 μm (A), 1.1 μm (B), and 2.0 μm (C) microspheres at ionic strength = 0.02 M and pH = 6.72 at fluid velocity of 8 m-day⁻¹ from the up-gradient, parallel column (reduced C₀), and the down-gradient columns.

surface heterogeneity exist that could lead to a distribution of deposition rate coefficients among the colloid population. Among these sources are significant variations in colloid size, variations in colloid surface charge, and variations in other colloid surface properties such as hydrophobicity.

Since they are easily measured, electrophoretic mobilities of the 1.0 μm microspheres were determined in the influent and effluent solutions using a zeta analyzer (ZetaPALS, Brookhaven Instruments Corporation, Holtsville, NY). Measurements were repeated 12 times at room temperature (22.5 °C). The average electrophoretic mobilities of the influent and effluent solution were -3.73 ± 0.018 and -4.12 ± 0.29

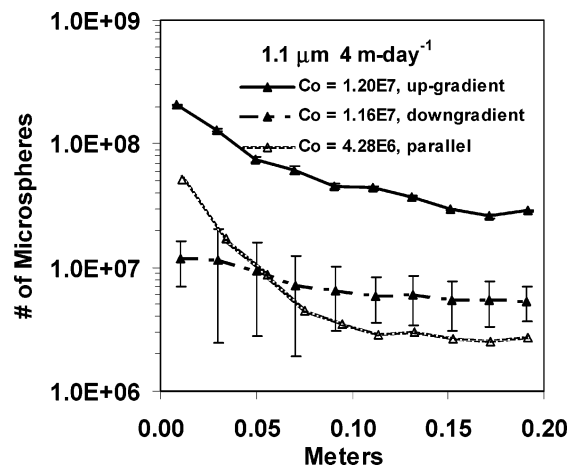


FIGURE 4. Retained profiles for 1.1 μm microspheres at ionic strength = 0.01 M and pH = 6.72 at fluid velocity of 4 m-day⁻¹ from the up-gradient, parallel column (reduced C₀), and the down-gradient columns.

$\times 10^{-8} \text{ m}^2 \text{ V}^{-1} \text{ s}^{-1}$, respectively. The slightly greater electrophoretic mobilities in the effluent relative to the influent solution (at one standard deviation) indicate that the average negative zeta potential among the colloid population increased with transport distance, consistent with the notion that the population became less sticky with increasing transport distance. Although the measured difference between the mean electrophoretic mobilities of the influent and effluent solution was only $0.39 \times 10^{-8} \text{ m}^2 \text{ V}^{-1} \text{ s}^{-1}$, it must be noted that the relationship between deposition rate coefficient and interaction potential may be exponential (e.g., ref 22). Hence, slight variations in electrophoretic mobilities among individuals within a population may yield wide distributions in deposition rate coefficients. However, we do not intend to assert that the colloid heterogeneity is strictly tied to surface charge. Other characteristics such as surface hydrophobicity (not examined in this study) may influence the resulting deposition rate coefficients.

Colloid size distributions in the influent and effluent solutions were also monitored using the zeta analyzer. Measurements were repeated 10 times at room temperature (22.5 °C). The average effective microsphere diameter of colloids in the influent and effluent solution was 1.07 ± 0.067 and $1.04 \pm 0.097 \mu\text{m}$, respectively. This insignificant difference in measured colloid sizes between the influent and effluent solutions indicate that colloid size was not a factor determining the preferential deposition of individual colloids within the population.

Recently, Bradford et al. (14–17) hypothesized that physical straining was an important contributor to the observed hyperexponential deviations from classic filtration theory when colloid:collector size ratios were greater than 0.005. The colloid:collector size ratios in our experiments ranged from 0.0002 to 0.0039, well below the recently suggested threshold of 0.005. Furthermore, the majority of retained colloids were re-entrained in response to elution with low ionic strength solution (described below), which is inconsistent with deposition via straining (e.g., refs 25 and 28). Therefore, it is highly unlikely that straining contributed to the deviations observed here.

Tufenkji and Elimelech (20) observed re-entrainment of the majority of retained colloids upon introduction of low ionic strength solution, demonstrating that the majority of retained colloids were associated with grain surfaces via the secondary energy minimum. These authors proposed that the fast-depositing colloids (sticky colloids) among the population were retained within secondary energy minima. To test their proposal, we examined the elution of the 0.5 μm

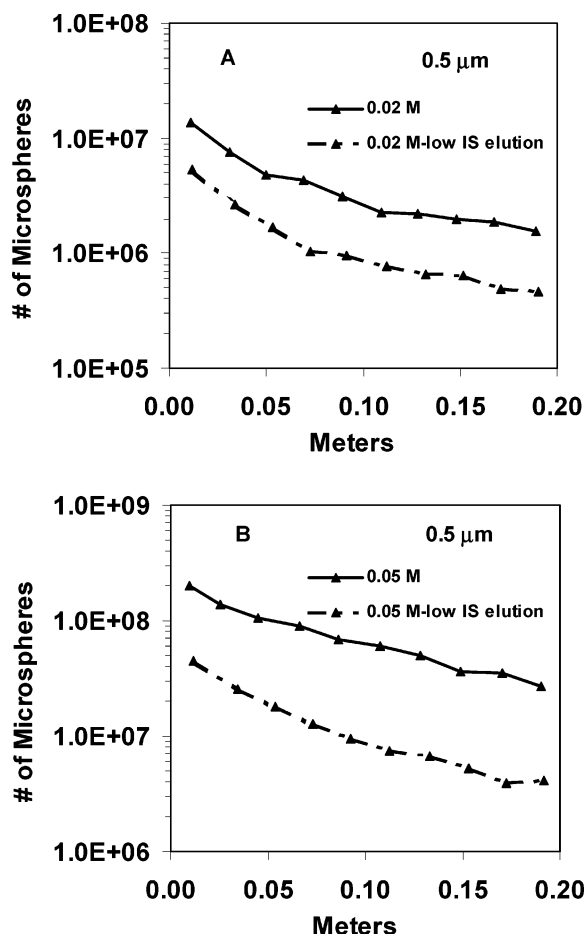


FIGURE 5. Retained profiles for $0.5\ \mu\text{m}$ microspheres with elution by high (0.02 for A or 0.05 M for B) and low ionic strength solution (0.0002 M) at ionic strength = 0.02 M (A) and 0.05 M (B) at fluid velocity of $4\ \text{m}\cdot\text{day}^{-1}$.

microspheres (at 0.02 and 0.05 M ionic strength, and pore water velocity = $4\ \text{m}\cdot\text{day}^{-1}$) from the porous media using low ionic strength solution (0.0002 M) and compared the resulting retained colloid profiles to parallel columns (same C_0) eluted with solution having the same ionic strength as the microsphere solution. The resulting retained colloid profiles are given in Figure 5 (A,B).

A significant fraction ($\sim 70\text{--}80\%$) of retained microspheres was released upon introduction of low ionic strength solution, indicating that the majority of deposited colloids were associated with grain surfaces via the secondary energy minimum. However, for both ionic strengths (0.02 and 0.05 M), the retained profiles displayed hyperexponential shapes that were identical to, but displaced in magnitude by about a factor of 4, relative to the pre-elution profiles (Figure 5A,B). This result indicates that microspheres were re-entrained evenly across the packed porous media and that deposition in secondary energy minima did not occur preferentially in the inlet end of the column but rather showed no spatial dependence. Hence, it is reasonable to conclude that the fast-depositing (sticky) fraction of the microsphere population did not preferentially deposit within secondary energy minima. It should be noted that the lowest detection concentration limit of the BD FACScan for the $0.5\ \mu\text{m}$ microspheres was $10^3\ \text{particles}\cdot\text{mL}^{-1}$. Although the percentage of microspheres retained after low ionic strength elution was small ($\sim 1.1\%$) (Figure 5A), the lowest concentration of supernatant samples from recovery of retained microspheres was still 100 times greater than that of the BD FACScan detection limit.

The profiles shown above indicate that hyperexponential deviation from classic filtration theory emanates from heterogeneity among the colloid population and that although the majority of retained colloids are associated with surfaces via secondary energy minima, deposition in secondary energy minima did not produce the observed hyperexponential deviations from classic filtration theory.

Acknowledgments

This material is based upon work supported by the National Science Foundation Hydrologic Sciences Program (EAR 0337258). Any opinions, findings, and conclusions or recommendations expressed in this material are those of the author(s) and do not necessarily reflect the views of the National Science Foundation. The authors wish to acknowledge three anonymous reviewers for their very helpful and insightful comments.

Supporting Information Available

Representative column experiment results and simulations using both single and distributed deposition rate coefficients. This material is available free of charge via the Internet at <http://pubs.acs.org>.

Literature Cited

- Yao, K. M.; Habibian, M. T.; O'Melia, C. R. Water and wastewater filtration: Concepts and applications. *Environ. Sci. Technol.* **1971**, *5* (11), 1105–1112.
- Rajagopalan, R.; Tien, C. Trajectory analysis of deep-bed filtration with the sphere-in-cell porous media model. *AIChE J.* **1976**, *22* (3), 523–533.
- Tufenkji, N.; Elimelech, M. Correlation equation for predicting single-collector efficiency in physicochemical filtration in saturated porous media. *Environ. Sci. Technol.* **2004**, *38*, 529–536.
- Tufenkji, N.; Redman, J. A.; Elimelech, M. Interpreting deposition patterns of microbial particles in laboratory-scale column experiments. *Environ. Sci. Technol.* **2003**, *37*, 616–623.
- Johnson, W. P.; Li, X.; Assemi, S. Hydrodynamic drag Influences deposition and re-entrainment dynamics of microbes and non-biological colloids during non-perturbed transport in porous media in the presence of an energy barrier to deposition. *Adv. Water Resour.* **2006**, doi:10.1016/j.advwatres.2006.05.020.
- Harter, T.; Wagner, S.; Atwill, E. R. Colloid transport and filtration of cryptosporidium parvum in sandy soils and aquifer sediments. *Environ. Sci. Technol.* **2000**, *34* (1), 62–70.
- Schijven, J. F.; Hoogenboezem, W.; Hassanizadeh, S. M.; Peters, J. H. Modeling removal of bacteriophages MS2 and PRD1 by dune recharge at Castricum, Netherlands. *Water Resour. Res.* **1999**, *35* (4), 1101–1111.
- Redman, J. A.; Estes, M. K.; Grant, S. B. Resolving macroscale and microscale heterogeneity in pathogen filtration. *Colloids Surf., A* **2001**, *191*, 57–70.
- Albinger, O.; Biesemeyer, B. K.; Arnold, R. G.; Logan, B. E. Effect of bacterial heterogeneity on adhesion to uniform collectors by monoclonal populations. *FEMS Microbiol. Lett.* **1994**, *124*, 321–326.
- Baygents, J. C.; Glynn, J. R., Jr.; Albinger, O.; Biesemeyer, B. K.; Ogden, K. L.; Arnold, R. G. Variation of surface charge density in monoclonal bacterial populations: implications for transport through porous media. *Environ. Sci. Technol.* **1998**, *32* (11), 1596–1603.
- Simoni, S. F.; Harms, H.; Bosma, T. N. P.; Zehnder, A. J. B. Population heterogeneity affects transport of bacteria through sand columns at low flow rates. *Environ. Sci. Technol.* **1998**, *32* (14), 2100–2105.
- Bolster, C. H.; Mills, A. L.; Hornberger, G.; Herman, J. Effect of intra-population variability on the long-distance transport of bacteria. *Ground Water* **2000**, *38* (3), 370–375.
- Redman, J. A.; Grant, S. B.; Olson, T. M.; Estes, M. K. Pathogen filtration, heterogeneity, and the potable reuse of wastewater. *Environ. Sci. Technol.* **2001**, *35* (9), 1798–1805.
- Bradford, S. A.; Yates, S. R.; Bettahar, M.; Simunek, J. Physical factors affecting the transport and fate of colloids in saturated porous media. *Water Resour. Res.* **2002**, *38* (12), 1327–1338.

- (15) Bradford, S. A.; Bettahar, M.; Simunek, J.; van Genuchten, M. T. Straining and attachment of colloids in physically heterogeneous porous media. *Vadose Zone J.* **2004**, *3*, 384–394.
- (16) Bradford, S. A.; Simunek, J.; Bettahar, M.; van Genuchten, M. T.; Yates, S. R. Modeling colloid attachment, straining, and exclusion in saturated porous media. *Environ. Sci. Technol.* **2003**, *37*, 2242–2250.
- (17) Bradford, S. A.; Simunek, J.; Bettahar, M.; Tadassa, Y. F.; van Genuchten, M. T.; Yates, S. R. Straining of colloids at textural interfaces. *Water. Resour. Res.* **2005**, *41*, doi:10.1029/2004WR003675.
- (18) Sakthivadivel, R. *Theory and mechanism of filtration of non-colloidal fines through a porous medium*; Hydraulic Engineering Laboratory, University of California: Berkeley, CA, 1966.
- (19) Sakthivadivel, R. *Clogging of a granular porous medium by sediment*; Hydraulic Engineering Laboratory, University of California: Berkeley, CA, 1969.
- (20) Tufenkji, N.; Elimelech, M. Breakdown of colloid filtration theory: role of the secondary energy minimum and surface charge heterogeneities. *Langmuir* **2005**, *21*, 841–852.
- (21) Johnson, W. P.; Li, X. Comment on breakdown of colloid filtration theory: role of the secondary energy minimum and surface charge heterogeneities. *Langmuir* **2005**, *21*, 10895–10895.
- (22) Li, X.; Scheibe, T. D.; Johnson, W. P. Apparent decreases in colloid deposition rate coefficient with distance of transport under unfavorable deposition conditions: a general phenomenon. *Environ. Sci. Technol.* **2004**, *38* (21), 5616–5625.
- (23) Zhang, P.; Johnson, W. P.; Scheibe, T. D.; Choi, K.; Dobbs, F. C.; Mailloux, B. J. Extended tailing of bacterial following breakthrough at the Narrow Channel focus area, Oyster, Virginia. *Water Resour. Res.* **2001**, *37*, 2687–2698.
- (24) Scheibe, T. D.; Wood, B. D. A particle-based model of size or anion exclusion with application to microbial transport in porous media. *Water Resour. Res.* **2003**, *39* (4), doi:10.1029/2001WR001223.
- (25) Tong, M.; Johnson, W. P. Excess colloid retention in porous media as a function of colloid size, fluid velocity, and grain angularity. *Environ. Sci. Technol.* **2006**, *40*, 7725–7731.
- (26) Li, X.; Zhang, P.; Lin, C. L.; Johnson, W. P. Role of hydrodynamic drag on microsphere deposition and re-entrainment in porous media under unfavorable conditions. *Environ. Sci. Technol.* **2005**, *39* (11), 4012–4020.
- (27) Johnson, W. P.; Tong, M. Observed and simulated fluid drag effects on colloid deposition in the presence of an energy barrier in an impinging jet system. *Environ. Sci. Technol.* **2006**, *40* (16), 5015–5021.
- (28) Brow, C.; Li, X.; Ricka, J.; Johnson, W. P. Comparison of microsphere deposition in porous media versus simple shear systems. *Colloids Surf., A* **2005**, *253*, 125–136.

Received for review May 18, 2006. Revised manuscript received October 25, 2006. Accepted October 30, 2006.

ES061202J